

Article

Structure and Technological Parameters' Effect on MISFET-Based Hydrogen Sensors' Characteristics

Boris Podlepetsky, Nikolay Samotaev *, Maya Etrekova  and Artur Litvinov

Micro- and Nanoelectronics Department, National Research Nuclear University MEPhI (Moscow Engineering Physics Institute), Kashirskoe Highway 31, 115409 Moscow, Russia

* Correspondence: nnsamotaev@mephi.ru

Abstract: The influence of structure and technological parameters (STPs) on the metrological characteristics of hydrogen sensors based on MISFETs has been investigated. Compact electrophysical and electrical models connecting the drain current, the voltage between the drain and the source and the voltage between the gate and the substrate with the technological parameters of the *n*-channel MISFET as a sensitive element of the hydrogen sensor are proposed in a general form. Unlike the majority of works, in which the hydrogen sensitivity of only the threshold voltage of the MISFET is investigated, the proposed models allow us to simulate the hydrogen sensitivity of gate voltages or drain currents in weak and strong inversion modes, taking into account changes in the MIS structure charges. A quantitative assessment of the effect of STPs on MISFET performances (conversion function, hydrogen sensitivity, gas concentration measurement errors, sensitivity threshold and operating range) is given for a MISFET with a Pd-Ta₂O₅-SiO₂-Si structure. In the calculations, the parameters of the models obtained on the basis of the previous experimental results were used. It was shown how STPs and their technological variations, taking into account the electrical parameters, can affect the characteristics of MISFET-based hydrogen sensors. It is noted, in particular, that for MISFET with submicron two-layer gate insulators, the key influencing parameters are their type and thickness. Proposed approaches and compact refined models can be used to predict performances of MISFET-based gas analysis devices and micro-systems.



Citation: Podlepetsky, B.; Samotaev, N.; Etrekova, M.; Litvinov, A. Structure and Technological Parameters' Effect on MISFET-Based Hydrogen Sensors' Characteristics. *Sensors* **2023**, *23*, 3273. <https://doi.org/10.3390/s23063273>

Academic Editor: Antonio Di Bartolomeo

Received: 16 February 2023
Revised: 14 March 2023
Accepted: 16 March 2023
Published: 20 March 2023



Copyright: © 2023 by the authors. Licensee MDPI, Basel, Switzerland. This article is an open access article distributed under the terms and conditions of the Creative Commons Attribution (CC BY) license (<https://creativecommons.org/licenses/by/4.0/>).

Keywords: MISFET; technological parameters; models; hydrogen sensor performances

1. Introduction

Many types of hydrogen sensors are used in fire–explosion safety and environmental monitoring systems [1]. The microminiaturization and intellectualization of such systems based on microtechnology and nanotechnology as well as improving their performance characteristics are the main trends of their development [2]. To develop the integrated hydrogen sensors and gas-analytic lab-on-chip systems, the sensitive elements must have technological compatibility with the elements of the integrated circuits. The capacitor and transistor elements based on metal–insulator–semiconductor (MIS) structures have good compatibility with the integrated circuits' elements [3].

Gas sensors based on MIS capacitors and field-effect transistors (MISFETs) have been studied by many investigators. A great contribution to the developments of gas-sensitive MIS devices has been made by the researchers at Linköping University since their first work in 1975 [4]. Works [5,6] described the gas sensitivity mechanisms, the kinetic modeling of hydrogen adsorption/absorption in thin films of catalytic metals and the formation of hydrogen atom dipoles in the metal–SiO₂ interfaces of MIS sensors. MIS sensors with different gate material (palladium [6], platinum and iridium [7]), with dielectric films SiO₂, Si₃N₄-SiO₂, TiO₂-SiO₂ and Ta₂O₅-SiO₂ have been investigated [8]. The semiconductors Si [4,7], GaAs [3,9] and SiC [10] were used in MIS gas sensors to detect the low concentrations of gases H₂ [6], NH₃ [7], H₂S [11], NO₂ [12] and CO [13]. The studies

have shown that performance characteristics of MISFET-based hydrogen sensors depend on technological parameters [8], electrical modes [14], chip temperature [15] and external factors (e.g., irradiation [16]).

Work on the study of the hydrogen effect on the properties of thin Pd films (less than 1 micron) began long before the appearance of real MISFET, and they are still ongoing. It has been shown that under the influence of various concentrations of hydrogen in the air, the partial pressure of the surrounding gases, the temperature and type of substrate, the thickness and deposition technology of the Pd film as a result of chemical reactions, changes in the structure, density and chemical composition of palladium films can occur [8]. As a result, under certain conditions of thermo-hydrogen exposure, Pd_xH_y and PdO compounds are formed in palladium films, and the films themselves can swell and peel off from the substrate [17]. These effects lead to irreversible and/or reversible changes in the electrical conductivity of the films and the work of the electron output from Pd [3], which is the physical principle of operation of some types of hydrogen sensors.

In addition to these effects, the following processes are considered in the models of hydrogen sensitivity of MIS capacitors and MISFET. Firstly, the hydrogen molecules adsorb on the surface of the Pd film and then dissociate into atoms. The hydrogen concentration in Pd is proportional to the concentration of adsorbed hydrogen molecules in Pd and hydrogen concentrations in air, as well as dependent on Pd temperature and the concentrations of other molecules [18]. Secondly, there is the diffusion of hydrogen atoms through the Pd film to the Pd–insulator interface [6,19]. Some hydrogen atoms form Pd_xH_y compounds, the concentration, structure and “lifetime” of which strongly depend on the chip temperature and hydrogen concentration [14]. Some hydrogen atoms penetrate to the boundary, with the dielectric either directly through the pores in the palladium film or via the tunnel mechanism through palladium grains (clusters) [5,11]. It is these atoms that form a polarized dipole layer of H in the Pd–insulator interface [6]. In work [20], based on modeling, doubts are expressed about the possibility of forming a dipole layer at the palladium–dielectric boundary. Third, there may be diffusion and drift protons in the insulator [21].

Thus, the hydrogen sensitivity of MIS devices depends on many factors. The simultaneous taking into account of all the factors is very difficult or not possible at all. In this article, the hydrogen sensitivity of the sensor characteristics was evaluated on the basis of a two-component physical model that takes into account possible changes in the work of the electron output from the gate material and changes in the MIS structure.

In recent years, based on nano- on micro-technologies, gas sensors with low sensitivity thresholds and low inertia have been developed. For example, new developments used nanostructured palladium films and Pd nanotubes [22], electrodeposited nanomaterials [23], nanoporous silicon thin films [24], integrated FET [25] and carbon nanotubes [26]. Microtechnologies, in combination with CMOS technologies [27,28], are used not only for the development of hydrogen and hydrogen-containing gas sensors [29], but also for the detection of other types of gases (e.g., CO [13,30] and NO₂ [12,31]). Note that sensor developments [13,26] are based on functionalized Single-Walled Carbon Nanotubes (SWNTs).

The researchers at National Research Nuclear University MEPhI have developed and investigated the number of discrete and integrated gas sensors (MIS capacitors, Pd and Pt resistors) with Pd (or Pt)-SiO₂-Si, Pd/Ti-SiO₂-Si, Pd (or Pt)-Ta₂O₅-SiO₂-Si structures. Experiments have demonstrated that MISFETs have the best performances compared to MIS capacitors and resistors. In addition, the integrated sensors, containing MISFET with a Pd(Ag)-Ta₂O₅-SiO₂-Si-structure (hereinafter referred to as TSE), possess the best stability and reproducibility of characteristics [21]. In recent years, we have investigated the metrological and operating characteristics of TSE (e.g., electrical modes [14], chip temperature [15] and irradiation [16]).

In this paper, we have investigated the influence of the structure and technological parameters (STPs) on the characteristics of MISFET hydrogen sensors in a general form,

and for TSE, based on refined compact models, allowing us to simulate the hydrogen sensitivity of gate voltages or drain currents in weak and strong inversion modes, taking into account changes in the work of the electron output from the gate material and charges in the MIS structure. A quantitative assessment of the effect of STP on the TSE conversion function, hydrogen sensitivity, gas concentration measurement errors, sensitivity threshold and operating range is given.

2. Materials and Methods

2.1. Initial Structure and Technological Parameters of TSE

The initial structure and technological parameters, which are considered unchanged when modeling sensor characteristics, included the dimensional parameters of the structural elements, the parameters of the semiconductor and the dielectric materials listed in Table 1. The STP values are determined using the specified materials, structure and topology of the TSE and are used to calculate the parameters C_0 , a and b of the TSE characteristic electrophysical models.

Table 1. Average values of the parameters of MISFETs and parameters of used models.

| Symbols | Parameters | Values |
|--|---|--|
| Parameters of semiconductor and dielectric materials | | |
| ϵ_1, ϵ_2 and ϵ_3 | relative permittivity of Ta ₂ O ₅ , SiO ₂ and Si | 25, 4 and 12 |
| N_A | concentration of acceptors in Si | $5 \times 10^{15} \text{ cm}^{-3}$ |
| μ_n | electron mobility in the channel | $200 \text{ cm}^2/(\text{V}\cdot\text{s})$ |
| Dimensions of structural elements | | |
| L and w | channel length and width | 10 μm and 3.2 mm |
| d_1 and d_2 | thicknesses of Ta ₂ O ₅ and SiO ₂ | 90 nm and 80 nm |
| d_m | thickness of the gate metal film | 70 nm |
| Constants and derived parameters | | |
| ϵ_0 | dielectric constant of vacuum | $8.85 \times 10^{-12} \text{ F/m}$ |
| k | Boltzmann constant | $1.38 \times 10^{-23} \text{ J/K}$ |
| q | electron charge | $1.6 \times 10^{-19} \text{ C}$ |
| d | thickness of the gate dielectric is $(d_1 + d_2)$ | 170 nm |
| ϵ | effective permittivity of the dielectric layer is $(d\epsilon_1\epsilon_2)/(\epsilon_1d_2 + \epsilon_2d_1)$ | 7.1 |
| C_0 | specific capacity of the dielectric $(\epsilon_0\epsilon)/d$ | 37 nF/cm^2 |
| a | charge parameter in Si is $(2q \epsilon_0 \cdot \epsilon_3 \cdot N_A)^{1/2}/C_0$ | $1.18 \text{ V}^{1/2}$ |
| b | specific steepness is $(\mu_n w C_0)/L$ | 2 mA/V^2 |
| Physical and electrical parameters | | |
| φ_{ms} | output work difference potential Pd–Si | $\varphi_{ms0} = 85 \text{ mV}$ |
| T | chip temperature | 400 K |
| φ_T | thermal potential (kT/q) at 400 K | 33 mV |
| φ_{gb} | the potential of the band gap in Si | 1.08 V |
| φ_{s0} | the potential of acceptors' level is $\varphi_T \ln(N_A/n_i)$ at 400 K | 0.21 V |
| φ_s | surface potential is $[\varphi(\text{SiO}_2 - \text{Si}) - \varphi_F]$ | 0.2 ... 0.8 V |
| Q_{te} and Q_{ss} | charge densities in the dielectric and in SiO ₂ – Si interface | $(5 \dots 100) \text{ nC/cm}^2$ |
| I_D | drain current | $(2 \dots 300) \mu\text{A}$ |
| V_D | voltage between the drain and the source | $(0.1 \dots 0.5) \text{ V}$ |
| V_G | voltage between the gate and the substrate | $(1 \dots 3) \text{ V}$ |
| Q_{te} and Q_{ss} | charge densities in the dielectric and in SiO ₂ – Si interface | $(5 \dots 100) \text{ nC/cm}^2$ |
| I_D | drain current | $(2 \dots 300) \mu\text{A}$ |
| V_D | voltage between the drain and the source | $(0.1 \dots 0.5) \text{ V}$ |
| V_G | voltage between the gate and the substrate | $(1 \dots 3) \text{ V}$ |

The errors in the calculations of electrophysical parameters depend on the errors of the STPs, which are determined using the technological standards or errors of the measuring

instruments, if the values of the STPs were determined experimentally. For example, if ε_3 is (12 ± 0.2) , w is (3.2 ± 0.02) mm, L is (10 ± 0.1) μm , μ_n is (200 ± 5) $\text{cm}^2/(\text{V}\cdot\text{s})$, N_A is $(5 \pm 0.02) \times 10^{15}$ cm^{-3} , then the relative errors of the parameters C_0 , a and b are equal to 3.5%, 4.5% and 8.7%, respectively. Denote the parameters with the symbol $p_k \in \{p_k\}$ ($k = 1, 2, \dots, 13$ in Table 2). In general, the absolute and relative errors of the parameters Δp_k and δp_k are equal to $|p_{kn} - p_k|$ and $(\Delta p_k/p_{kn}) \times 100\%$, respectively. The value of p_{kn} is the desired (nominal) value of parameter p_k or its average value, if this parameter was determined experimentally from a set of measured values.

Table 2. The effect of STP p_k on the components of TSE models.

| k | STP | Components of TSE Models |
|----|----------------------------------|--|
| 1 | film production technologies | Pd |
| 2 | | Ta ₂ O ₅ |
| 3 | | SiO ₂ |
| 4 | film thicknesses | Pd (d_M) |
| 5 | | Ta ₂ O ₅ (d_1) |
| 6 | | SiO ₂ (d_2) |
| 7 | acceptor concentration | (N_A) |
| 8 | channel length | (L) |
| 9 | channel width | (w) |
| 10 | electron mobility in the channel | (μ_n) |
| 11 | relative dielectric permittivity | Ta ₂ O ₅ (ε_1) |
| 12 | | SiO ₂ (ε_2) |
| 13 | | Si (ε_3) |

The absolute errors of Δp_k depend on the film manufacturing technologies (for parameters with indices $k \in \{1; 2; 3; 4; 5; 6\}$), on photolithography technologies (for p_8, p_9), on methods of estimating their thicknesses (for parameters with indices $k \in \{4; 5; 6\}$) and on the type and structure of the materials (for parameters with indexes $k \in \{11; 12; 13\}$). Typically, the values of Δw and ΔL are in the range of 0.1 to 0.5 microns, and values $\Delta d \in [5 \text{ nm}; 15 \text{ nm}]$ depend on d . The relative errors δw and δL are in the range from 0.002%...0.01% to 1.1%...5%. For specific technologies of the semiconductor wafers and dielectric films production, the relative errors $\delta\varepsilon_1, \delta\varepsilon_2, \delta\varepsilon_3, \delta\mu_n$ and δN_A usually do not exceed 2%. The relative errors of δd_1 and δd_2 are in the range of $\delta d_{\min} \in [2\%; 10\%]$ to $d_{\max} \in [7.5\%; 30\%]$ and are the maximum for the STPs. Consequently, the thicknesses d_1 and d_2 , the dimension of which will be determined in nm, can be considered the most critical STP.

2.2. Metrological Characteristics of TSE

To assess the influence of various factors on the characteristics of the sensors and systems being developed based on MISFETs, simulation modeling can be used, which is considered a fast and inexpensive method compared to full-scale tests of sensors with various STPs. In simulation modeling, the type, structure and values of STPs and the parameters of the models are chosen arbitrarily. In this paper, the characteristics of the TSE with the parameters specified in Table 1 were studied.

A fragment of the structure, the schematic designation of the n -channel TSE and a potentiometric circuit of its embedding for measuring the gas concentration C are shown in Figures 1 and 2.

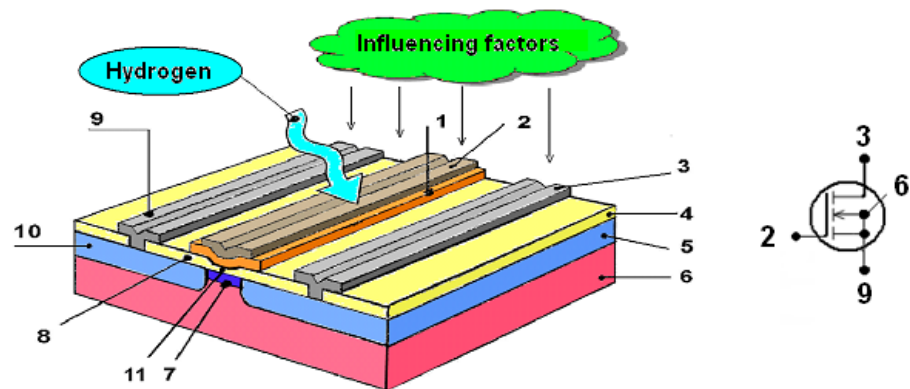


Figure 1. The structure and the schematic designation of TSE: 1 is gas-sensitive film, 2 is metal gate, 3 and 9 are drain and source contacts, 4 and 8 are passivating films, 5 and 10 are drain and source, 6 is substrate, 7 is channel, 11 is thin gate dielectric.

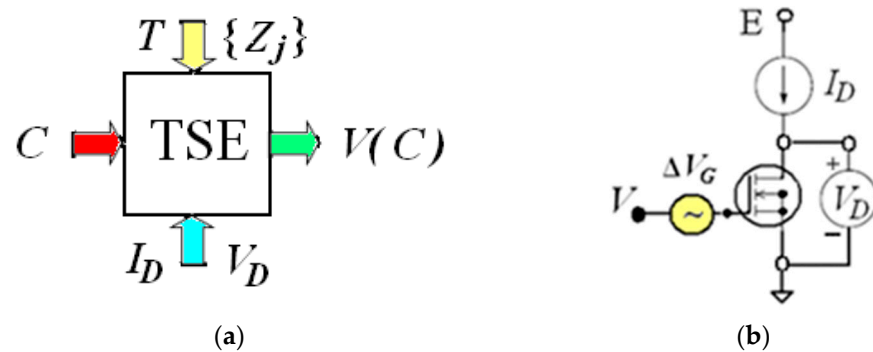


Figure 2. (a) The input informative parameter is the gas concentration C ; the output informative parameter is the voltage of the output signal V ; the operating chip temperature is T ; the parameters of the electrical mode of the circuit are the current I_D and the voltage V_D ; external influencing factors $\{Z_j\}$ are molecules of other gases, temperature, humidity and radiation background of the environment. (b) The circuit for measuring the dependence V as function of C .

The main metrological characteristics of TCE include: conversion function (dependence V as function of C); differential S_d and integral S sensitivities being equal to dV/dC and $\Delta V/\Delta C$; absolute ΔC and relative δC errors of measurement C ; the sensitivity threshold C_{th} ; minimum relative error δC_{min} ; the boundaries of the working range C_1 and C_2 , limited by a given error δC_{max} and finally C_{max} .

As previous studies [16,21] have shown, the conversion function of a TSE can be represented in general form as $V(C)$ is $[V_0 - \Delta V(C)]$, where the initial value of V (at $C = 0$) is equal to V_0 . In general, the output signals V of MISFETs-based sensors are formed as a result of the embedding of one or more transistors in various measurement circuits. In this paper, the main components of the models are determined using experimental studies of one TSE in the mode with a constant current I_D and the voltage V_D as shown in Figure 2b. In this case,

$$V(C) = V_G(C) = V_{G0} - \Delta V_G(C) \text{ and } S_d = dV_G/dC, \quad (1)$$

$$V_{G0}(\varphi_s) = \varphi_s + a \cdot \{\varphi_s + \varphi_T \cdot \exp[(\varphi_s - 2\varphi_{s0})/\varphi_T]\}^{1/2} + \varphi_{ms0} - [Q_{te0} + Q_{ss}(\varphi_s)]/C_0. \quad (2)$$

For modeling the characteristics of TSE sensors, the following expression can be used to approximate the conversion function in the range of hydrogen concentrations from 0.005 vol.% to 1.5 vol.% [16]:

$$\Delta V_G(C) = \Delta Q_{te}(C)/C_0 - \Delta \varphi_{ms}(C) = \Delta V_m \cdot [1 - \exp(-k_C \cdot C)] > 0. \quad (3)$$

Then, the sensitivity of S_d is equal to $[-k_C \cdot \Delta V_m \cdot \exp(-k_C \cdot C)]$. The maximum relative error of measuring the gas concentration δC in the general case is represented as

$$\delta C = 100\% \times \Delta C / C = 100\% \times [\Delta(C) \cdot |S_d| + \Delta V + \Delta(V)] / (C |S_d|), \quad (4)$$

where $\Delta(C)$ is the absolute error of the specified gas concentration during sensor calibration, ΔV is the error voltage measurements and $\Delta(V)$ being equal to $\Delta(\Delta V_G)$ is the absolute voltage error associated with an absolute error of the parameter p_k and is approximately equal to $[dV_G/dp_k] \cdot \Delta p_k$. Then, after sensor calibration the sensitivity threshold C_{th} is $(\Delta V / |S_{dmax}|)$, minimum relative error is δC_{min} and the boundaries of the working range C_1 and C_2 can be determined as solutions of Equations (5) and (6). The value of δC_{min} is δC (at C is C^*), where C^* is the solution of the following equation:

$$d(\delta C) / dC = 0. \quad (5)$$

The values of C_1 and C_2 are solutions of Equation (6) with respect to C at a given δC_{max} greater than δC_{min} :

$$\delta C_{max} = 100\% \times [\Delta(C) |S_d| + \Delta V + \Delta(V)] / (C |S_d|), \quad (6)$$

$$C_{max} = (1/k_C) \cdot \ln(\Delta V_m / \Delta V). \quad (7)$$

These transcendental equations will be solved using numerical methods. The testing n -channel MISFET based on the Pd-Ta₂O₅-SiO₂-Si structure was fabricated on a single chip ($2 \times 2 \text{ mm}^2$) together with a (p - n) junction temperature sensor and heater resistor by means of conventional n -MOS technology. Technological processes are detailed and presented in [14,21].

3. Results

3.1. Influence of Film Manufacturing Technology and Thicknesses on the Components of the Conversion Function

The experimental studies demonstrated that the MISFET hydrogen sensitivity depends on several effects, which occur in regions of the (ambient gas)–metal–dielectric structure. The probability of various effects depends on the following factors: chip temperature; partial pressure of hydrogen; material, chemical composition, structure, manufacturing technology and thickness of the gate film and the pressure of the gas medium [4,13,18,22,23]. The presence of a large number of influencing factors complicates and/or make it impossible in principle to simulate the influence of the material, the technology of production and the thickness of the shutter film on the metrological characteristics of MISFETs. The degree of this influence can only be determined experimentally. The morphology (crystalline, polycrystalline, amorphous, nanoparticles, etc.) of palladium films may affect the hydrogen sensitivity of sensors based on Pd film resistors or MIS structures as shown, for example, in [21,22].

Basically, the deposition technology and thickness of metal film d_m can affect the conversion function components $\Delta Q_{te}(C)$ and $\Delta \varphi_{ms}(C)$. In the investigated TSE Pd film (d_m is $70 \pm 5 \text{ nm}$) was prepared using laser evaporation in vacuum $2 \cdot 10^{-3} \text{ Pa}$ in the substrate's temperature range of 300–400 °C. For this technology, at thicknesses d_m that is less than 80 nm, the palladium film has a porous structure. Therefore, it can be assumed that the hydrogen sensitivity and response time will be independent of d_m and of its deviations Δd_m from the nominal values of d_{mn} . For other technologies (for example, with thicknesses of nanostructured Pd films less than 30 nm), the response time decreased, and the sensitivity can be increased at low concentrations (~5–50 ppm) with a decrease in d_m [32]. Quantitative analysis of the effect of the Pd films' characteristics on the hydrogen sensitivity of the TSE requires special experimental studies, which have not been observed in this work.

Deposition technologies and the thicknesses of dielectric films d_1 and d_2 can affect the conversion function components V_{G0} and ΔV_m , which according to (2) and (3) are inversely proportional to specific capacity C_0 :

$$V_{G0} = \varphi_s + 0.085 + \{41 \cdot [\varphi_s + 0.033 \cdot \exp((\varphi_s - 0.42)/0.033)]^{1/2} - 5\} / C_0 \text{ (V)}, \quad (8)$$

$$\Delta V_m = \Delta Q_{tem} / C_0 - \Delta \varphi_{msm} = 15 / C_0 + 0.11 \text{ (V)}, \quad (9)$$

$$C_0 = (\varepsilon_0 \varepsilon_1 \varepsilon_2) / (\varepsilon_1 d_2 + \varepsilon_2 d_1), \quad (10)$$

where in engineering physical models (8) and (9), the dimensions of the potentials are the volts, charge density is nC/cm^2 , capacitance is nF/cm^2 and thicknesses is nm. With an increase in the hydrogen concentration, the work of the electron output from Pd decreases, and therefore you have a negative value $\Delta \varphi_{ms}(C)$ [3]. The absolute ΔC_0 and relative δC_0 being equal to $100\% \times \Delta C_0 / C_0$ errors for C_0 are, respectively, equal to:

$$\Delta C_0 = \varepsilon_0 [\varepsilon_2 d_1 (\Delta \varepsilon_1 \cdot \varepsilon_2 + 2 \Delta \varepsilon_2 \cdot \varepsilon_1) + \varepsilon_1 d_2 (\Delta \varepsilon_2 \cdot \varepsilon_1 + 2 \Delta \varepsilon_1 \cdot \varepsilon_2) + \varepsilon_1 \cdot \varepsilon_2 (\Delta d_2 \cdot \varepsilon_1 + \Delta d_1 \cdot \varepsilon_2)] / (\varepsilon_1 d_2 + \varepsilon_2 d_1)^2, \quad (11)$$

$$\delta C_0 = [\delta \varepsilon_1 (2 \varepsilon_1 d_2 + \varepsilon_2 d_1) + \delta \varepsilon_2 (2 \varepsilon_2 d_1 + \varepsilon_1 d_2) + \delta d_2 \cdot \varepsilon_1 d_2 + \delta d_1 \cdot \varepsilon_2 d_1] / (\varepsilon_1 d_2 + \varepsilon_2 d_1), \quad (12)$$

where $\Delta \varepsilon_1$, $\Delta \varepsilon_2$, Δd_1 and Δd_2 and $\delta \varepsilon_1$, $\delta \varepsilon_2$, δd_1 and δd_2 are the absolute and relative errors of the corresponding values. For the values, ε_1 is 25 and ε_2 is 4, and the dependences of the components C_0 and δC_0 on thicknesses of d_2 at different values of d_1 are shown in Figure 3.

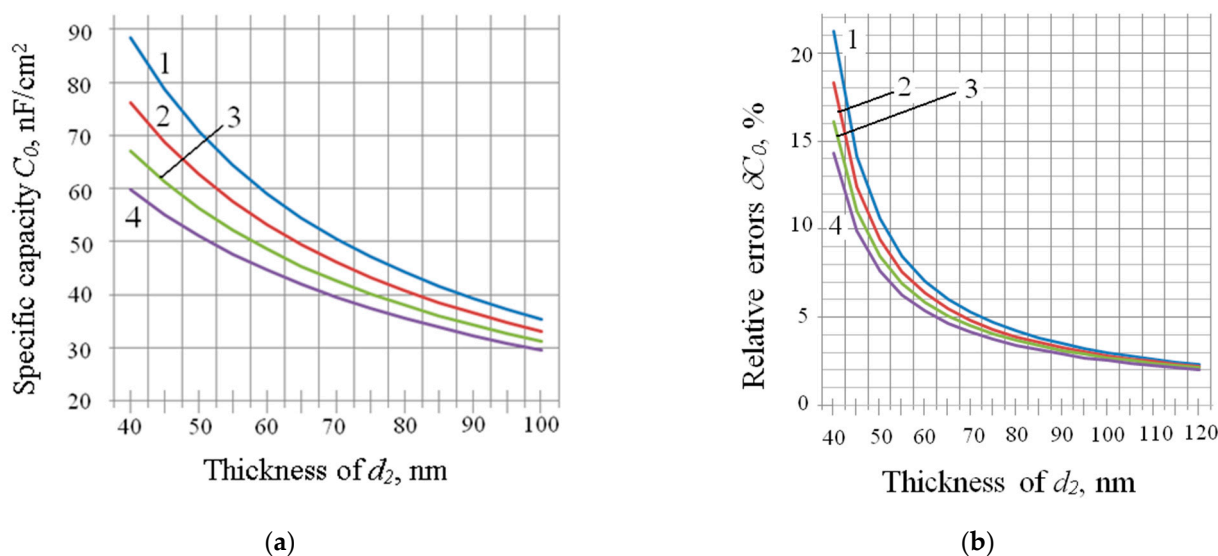


Figure 3. (a,b) are dependences $C_0(d_2)$ and $\delta C_0(d_2)$ at d_1 : 1 \rightarrow 0 nm; 2 \rightarrow 40 nm; 3 \rightarrow 80 nm; 4 \rightarrow 120 nm.

In the process of forming metal and dielectric films at a constant temperature T_p of the silicon wafer (substrate), their thicknesses depend on the time of the process t and on the temperature-dependent growth rate of the film v_i . For example, when creating a SiO_2 film via silicon oxidation in dry oxygen, the dependence of $d_2(t)$ for various T_p is shown in Figure 4 (based on Figure 8a in [32]). At the initial stage of silicon oxidation (up to d_2 is about 30 nm), the thickness of the SiO_2 film is proportional to the oxidation time t ; with further oxidation, the thickness of d_2 is proportional to $(t)^{1/2}$. If the oxidation of silicon in dry oxygen is carried out at a temperature of 1100 °C, then the thickness d_2 is $v_1 \cdot t$ (nm) at $t \in [0; 10 \text{ min}]$ and $d_2 = 30 + v_2 \cdot (t)^{1/2}$ (nm) when the t is greater than 10 min, where v_1 and v_2 are equal to 4.0 nm/min and $8.5 \text{ nm} \cdot \text{min}^{1/2}$; $[t]$ is min.

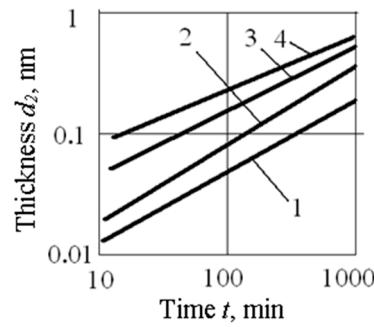


Figure 4. Dependence of the SiO₂ film thickness d_2 on the oxidation time t in dry oxygen at temperatures: 1 → 900 °C; 2 → 1000 °C; 3 → 1100 °C; 4 → 1200 °C.

The error δd_2 is $(\delta v_2 + 100\% \times \Delta t/t)$ or δd_2 is $(\delta v_2 + 50\% \times \Delta t/(t)^{1/2})$, where δv_2 depends on the dispersion of the plate temperature ΔT_p . The value of Δt is determined by the time parameters of the temperature response $T_p(t)$ when the plate is introduced into the core with the constant temperature and partial pressure of oxygen, or by the time parameters of establishing a constant partial pressure of oxygen after oxygen is introduced into the placement zone of the plate heated to the operating temperature T_p and the time of oxygen pressure drop. Usually, $\delta v_2 < 0.5\%$ and $\Delta t \in (0.5; 2)$ min. For a given thickness d_2 , the error δd_2 can be estimated as δd_2 being less than the value of $[0.5\% + 425\Delta t/(d_2 - 30)]$. For example, if d_2 is 50 nm and Δt is 30 s, then the value of $\delta d_2 < 11.1\%$, and if d_2 is 80 nm and Δt is 30 s, then the value of $\delta d_2 < 4.75\%$.

Thus, the thicknesses and dielectric permittivities of dielectric films determine the capacitance C_0 , which can be considered a key parameter affecting the TSE conversion function.

3.2. Influence of Material's Parameters and Topological Dimensions of Elements on Conversion Function Components

The material's parameters (ϵ_3 , N_A , μ_n) and topological dimensions (L , w) affect parameters a and b , which depend on the value of C_0 . According to (2), the conversion function component V_{G0} depends on the variables parameters a and φ_s . Then, the absolute error ΔV_{G0} with small deviations Δa and $\Delta \varphi_s$ from their average values can be presented as:

$$\Delta V_{G0} = (\partial V_{G0}/\partial \varphi_s)\Delta \varphi_s + (\partial V_{G0}/\partial a)\Delta a = 0.01 \cdot (K_\varphi \cdot \varphi_s \cdot \delta \varphi_s + K_a \cdot a \cdot \delta a), \quad (13)$$

$$K_\varphi = 1 + 0.5a(1 + \exp m)/(\varphi_s + \varphi_T \cdot \exp m)^{1/2}; K_a = (\varphi_s + \varphi_T \cdot \exp m)^{1/2}; m = (\varphi_s - 2\varphi_{s0})/\varphi_T. \quad (14)$$

Parameter a depends on values of ϵ_3 , N_A and C_0 , and the potential φ_s depends on the given values of I_D and V_D . According to the simplified TSE electrical model [15], the dependence $I_D(V_G)$ at $\varphi_s > 2\varphi_{s0}$ has two sections: parabolic when $I_D \in [I_{D0}; I_{D1}]$ and $\varphi_s \in [2\varphi_{s0}; \varphi_{s1}]$, and linear when value of I_D is greater than I_{D1} being equal to $(I_{D0} + 0.5bV_D^2)$. In principle, the entire range of changes in the drain current I_D and gate voltage V_G corresponding to the inversion mode can be used to measure the hydrogen concentration. Usually, the values of the set current are within the error range: I_D is $I_{Dn} \pm \Delta I_D$.

In practice, the electric mode of strong inversion (at $\varphi_s > \varphi_{s1}$) is chosen, in which the measurement errors ΔV_{G0} and δC are minimal. For example, when V_D is 0.2 V (I_{D1} is 42 μA) and I_D is equal to (20 ± 2) μA , the value of V_{G0} is (1.16 ± 0.01) V, and when I_D is equal to (100 ± 2) μA , the value of V_{G0} is (1.25 ± 0.005) V. Then, the values of I_D and fluctuations of $\Delta \varphi_s$ are represented as:

$$I_D = b \cdot \{a \cdot V_D \cdot [(\varphi_s + \varphi_T \exp m)^{1/2} - \varphi_s^{1/2}] - 0.5V_D^2\}; \Delta \varphi_s \approx 2\Delta I_D \cdot (\varphi_s + \varphi_T \exp m)^{1/2} / [a \cdot b \cdot V_D \cdot (1 + \exp m)]. \quad (15)$$

The dependences of the potential φ_s on the current I_D at different V_D and on values of V_{G0} at different C_0 are shown in Figure 5. The relative errors of conversion function components a and b are equal to:

$$\delta a = \delta C_0 + 0.5(\delta \varepsilon_3 + \delta N_A) = 4.5\% \text{ and } \delta b = \delta C_0 + \delta \mu_n + \delta w + \delta L = 8.7\%. \quad (16)$$

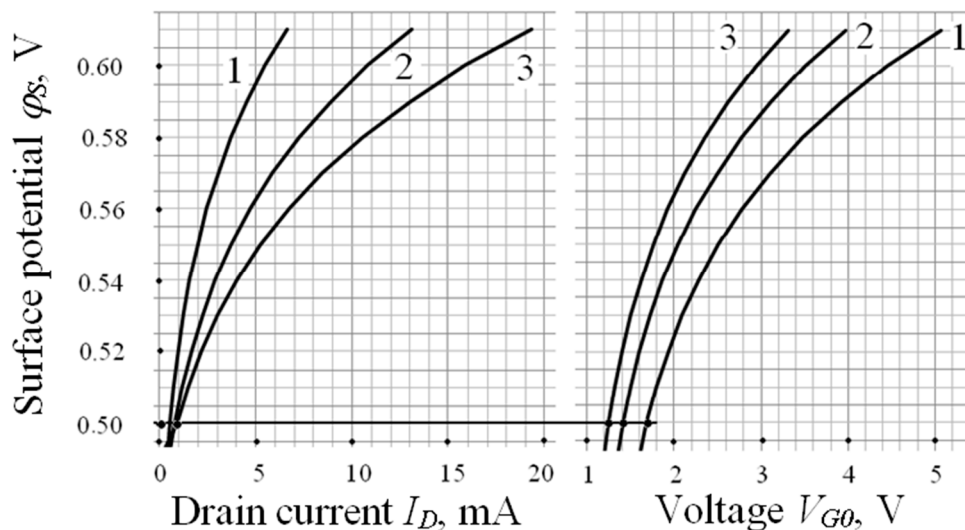


Figure 5. Dependences of values φ_s on the current I_D at different V_D (1 → 0.1 V; 2 → 0.2 V; 3 → 0.3 V), and on values of V_{G0} at different C_0 (1 → 30 nF/cm²; 2 → 40 nF/cm²; 3 → 50 nF/cm²).

Quantitative values of a and b are given for the investigated TSE. Average values of the parameters of the conversion function for different C_0 and (w/L) are presented in Table 3. As an example, Figure 5 shows the coordinates of the points corresponding to the values V_{G0} being equal to 1.2 V, 1.4 V and 1.7 V for different V_D and a given drain current of 1 mA.

Table 3. Average values of parameters for different C_0 and (w/L) at I_D is 0.1 mA and V_D is 0.2 V.

| Parameters → ↓ C_0 , nF/cm ² | δC_0 , % | a , V | δa , % | w/L Is 0.003 | | | w/L Is 0.006 | | |
|--|------------------|---------|----------------|-------------------------|----------------|----------------------|-------------------------|----------------|----------------------|
| | | | | b , mA/V ² | δb , % | ΔV_{G0} , mV | b , mA/V ² | δb , % | ΔV_{G0} , mV |
| 30 | 2.1 | 1.37 | 3.1 | 1.62 | 7.3 | 6 | 3.24 | 7.0 | 3 |
| 40 | 3.6 | 1.02 | 4.6 | 2.16 | 8.8 | 4.6 | 4.32 | 8.5 | 2.3 |
| 50 | 5.5 | 0.82 | 6.5 | 2.70 | 10.4 | 3.7 | 5.4 | 10.1 | 1.8 |

3.3. Influence of Specific Capacity on the Main Metrological Characteristics of TSE

The quantitative assessment of the effect of STPs on the initial value of the output signal, hydrogen sensitivity, absolute and relative errors in measuring gas concentration, the sensitivity threshold, the maximum concentration and the hydrogen concentration range for a given maximum relative error is given. The calculations used engineering physical models obtained on the basis of selected electrophysical and electrical models. The dependences of $\delta C(C)$ and the average values of metrological characteristics for different C_0 are presented in Figure 6 and in Table 4.

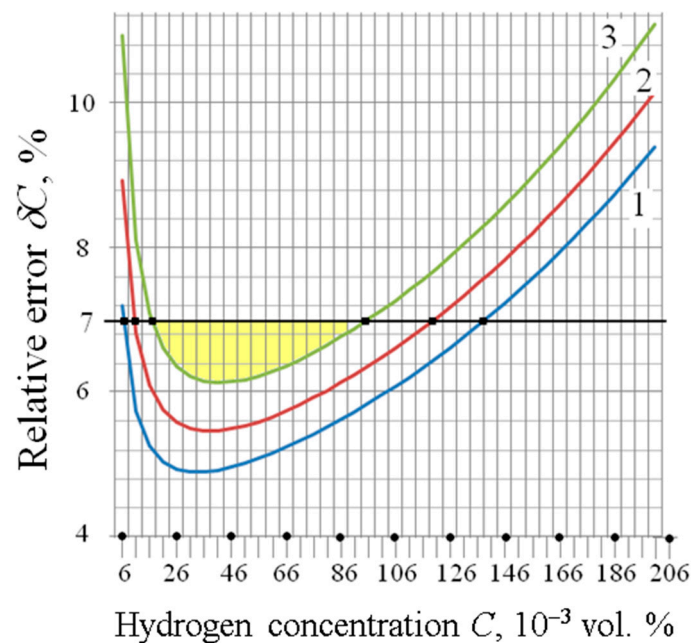


Figure 6. Dependence of $\delta C(C)$ for different C_0 : 1 \rightarrow 30 nF/cm²; 2 \rightarrow 40 nF/cm²; 3 \rightarrow 50 nF/cm². The values of C_1 and C_2 correspond to the square points on the curves. The color indicates the working area for the curve corresponding to the capacity of 50 nF/cm².

Table 4. Average values of metrological characteristics for different C_0 at δC_{max} being equal to 7%.

| MC \rightarrow $\downarrow C_0, \text{nF/cm}^2$ | $V_{G0},$ V | $\Delta V_m,$ V | $k_{Cr},$ 1/(vol.%) | $S_{dmax},$ V/(vol.%) | $\delta C_{min},$ % | $C_{thr},$ ppm | $C_1,$ ppm | $C_2,$ ppm | $C_{max},$ ppm |
|---|----------------|--------------------|------------------------|--------------------------|------------------------|-------------------|---------------|---------------|-------------------|
| 30 | 1.55 | 0.61 | | 4.88 | 4.9 | 2.0 | 50 | 1410 | 8016 |
| 40 | 1.52 | 0.42 | 8 | 3.36 | 5.5 | 2.9 | 90 | 1210 | 7550 |
| 50 | 1.48 | 0.32 | | 2.56 | 6.1 | 3.9 | 160 | 960 | 7210 |

4. Discussion

The analysis of the data obtained allows us to draw the following conclusions.

- All the considered STPs of the TSE (p_k in Table 2) affect the components of the conversion function on which the main metrological characteristics depend.
- The deposition technology and thickness of the metal film d_m can affect the conversion function components $\Delta Q_{te}(C)$ and $\Delta \varphi_{ms}(C)$ on which the sensor's hydrogen sensitivity and the response time depend. A quantitative analysis of the effect of the Pd films technological characteristics on TSE hydrogen sensitivity requires special experimental studies. In the investigated TSE, the Pd film has a porous structure. Therefore, it can be assumed that the hydrogen sensitivity and response time will be independent of d_m and of its deviations Δd_m from the nominal values of d_{mn} .
- The values of V_{G0} and ΔV_{G0} depend on N_A , C_0 and the given electrical parameters I_D and V_D . With the growth of I_D and V_D , the error ΔV_{G0} decreases. As a result of the calibration of the measuring device, the zero error is determined by the error ΔV_{G0} or the instrumental error of the voltage measurement ΔV (in the examples considered, ΔV is 1 mV).

5. Conclusions

Refined compact electrophysical and electrical models are proposed that link the drain current, the voltage between the drain and the source, the voltage between the gate and the

substrate with the structure and technological parameters (STPs) of an *n*-channel MISFET as a sensitive element of a hydrogen sensor (TSE). The method of the analytical assessment of the effect of STPs on the main metrological characteristics of a TSE is proposed. A qualitative assessment is given of the influence of the metal gate film manufacturing technology, the technology of manufacturing the gate dielectric films and their thicknesses, the concentration of impurities in the semiconductor, the length and width of the channel and the mobility of electrons in the channel on the metrological characteristics of TCE.

Using the example of a TSE with a Pd-Ta₂O₅-SiO₂-Si structure, manufactured according to a specific technology, a quantitative assessment of the effect of STPs on the initial value of the output signal, hydrogen sensitivity, absolute and relative errors in measuring gas concentration, the sensitivity threshold and the hydrogen concentration range for a given maximum relative error is given. The calculations used engineering physical models obtained on the basis of selected electrophysical and electrical models.

The degree of influence of each STP and their errors on the components of the conversion function and the main metrological characteristics of a TSE is shown. It has been established that for a specific technology of manufacturing TSEs (in particular, for MISFET with submicron two-layer gate insulators), the key influencing parameters are their type and thickness. Proposed approaches and models can be used to predict performances of MISFET-based gas analysis devices and micro-systems and also to solve the inverse problem determining the STPs according to the specified metrological characteristics.

In contrast to works [22,29], in which structures with ultrathin single-layer dielectric films were studied, this work shows the significant effect on the hydrogen sensitivity of sensors of submicron thicknesses of MISFET dielectrics.

Author Contributions: Conceptualization, B.P.; data curation, B.P. and M.E.; formal analysis, A.L.; funding acquisition, N.S.; investigation, M.E. and A.L.; methodology, B.P.; project administration, N.S.; resources, A.L.; supervision, N.S.; validation, M.E.; writing—original draft, B.P.; writing—review and editing, N.S. All authors will be informed about each step of manuscript processing including submission, revision, revision reminder, etc. via emails from our system or assigned Assistant Editor. All authors have read and agreed to the published version of the manuscript.

Funding: This work was supported by a grant from the Russian Science Foundation No. 18-79-10230.

Institutional Review Board Statement: Not applicable.

Informed Consent Statement: Not applicable.

Data Availability Statement: Data sharing not applicable.

Conflicts of Interest: The authors declare no conflict of interest. The funders had no role in the design of the study; in the collection, analyses, or interpretation of the data; in the writing of the manuscript; or in the decision to publish the results.

References

1. Hübert, T.; Boon-Brett, L.; Black, G.; Banach, U. Hydrogen sensors—A review. *Sens. Actuators B* **2011**, *157*, 329–352. [[CrossRef](#)]
2. Hong, S.; Wu, M.; Hong, Y.; Jeong, Y.; Jung, G.; Shin, W.; Park, J.; Kim, D.; Jang, D.; Lee, J.H. FET-type gas sensors: A review. *Sens. Actuators B* **2020**, *330*, 129240. [[CrossRef](#)]
3. Tejaswini, S.; Paresh, K. Work Function-Based MOS Hydrogen Sensor and its Functionality: A Review. *Adv. Mater. Interfaces* **2021**, *8*, 2100649.
4. Lundström, I.; Shivaraman, S.; Svensson, C.; Lundkvist, L. A hydrogen-sensitive MOS field-effect transistor. *Appl. Phys. Lett.* **1975**, *26*, 55–57. [[CrossRef](#)]
5. Lundström, I. Hydrogen sensitive MOS-structures, Part I: Principles and applications. *Sens. Actuators* **1981**, *1*, 423–426. [[CrossRef](#)]
6. Lundström, I.; Armgarth, M.; Spetz, A.; Winquist, F. Gas sensors based on catalytic metal-gate field-effect devices. *Sens. Actuators* **1986**, *3–4*, 399–421. [[CrossRef](#)]
7. Spetz, A.; Helmersson, U.; Enquist, F.; Armgarth, M.; Lundström, I. Structure and ammonia sensitivity of thin platinum or iridium gates in metal–oxide–silicon capacitors. *Thin Solid Film.* **1989**, *177*, 77–93. [[CrossRef](#)]
8. Lundström, I.; Sundgren, H.; Winquist, F.; Eriksson, M.; Krants-Rülcker, C.; Lloyd-Spets, A. Twenty-five years of field effect gas sensor research in Linköping. *Sens. Actuators B Chem.* **2007**, *121*, 247–262. [[CrossRef](#)]

9. Lin, K.W.; Cheng, C.C.; Cheng, S.Y.; Yu, K.H.; Wang, C.K.; Chuang, H.M.; Liu, W.C. A novel Pd/oxide/GaAs metal–insulator–semiconductor field-effect transistor (MISFET) hydrogen sensor. *Semicond. Sci. Technol.* **2001**, *16*, 997–1001. [[CrossRef](#)]
10. Andersson, M.; Pearce, R.; Lloyd-Spetz, A. New generation SiC based field effect transistor gas sensors. *Sens. Actuators B Chem.* **2013**, *179*, 95–106. [[CrossRef](#)]
11. Kalinina, L.; Litvinov, A.; Nikolaev, I.; Samotaev, N. MIS-Field Effect Sensors for low concentration of H₂S for environmental monitoring. *Procedia Eng.* **2010**, *5*, 1216–1219. [[CrossRef](#)]
12. Yaqoob, U.; Younis, M.I. Chemical Gas Sensors: Recent Developments, Challenges, and the Potential of Machine Learning—A Review. *Sensors* **2021**, *21*, 2877. [[CrossRef](#)] [[PubMed](#)]
13. Ren, Q.; Cao, Y.Q.; Arulraj, D.; Liu, C.; Wu, D.; Li, W.M.; Li, A.D. Resistive-Type Hydrogen Sensors Based on Zinc Oxide Nanostructures. *J. Electrochem. Soc.* **2020**, *167*, 067528. [[CrossRef](#)]
14. Podlepetsky, B.; Nikiforova, M.; Kovalenko, A. Chip temperature influence on characteristics of MISFET hydrogen sensors. *Sens. Actuators B* **2018**, *254*, 1200–1205. [[CrossRef](#)]
15. Podlepetsky, B.; Kovalenko, A.; Samotaev, N. Influence of electrical modes on performance of MISFET hydrogen sensors. *Sens. Actuators B* **2017**, *248*, 1017–1022. [[CrossRef](#)]
16. Podlepetsky, B. Effect of irradiation on hydrogen sensors based on MISFET. *Sens. Actuators B* **2017**, *238*, 1207–1213. [[CrossRef](#)]
17. Gurlo, A.; Clarke, D. High-Sensitivity Hydrogen Detection: Hydrogen-Induced Swelling of Multiple Cracked Palladium Films on Compliant Substrates. *Angew. Chem. Int. Ed.* **2011**, *50*, 10130–10132. [[CrossRef](#)] [[PubMed](#)]
18. Eriksson, M.; Lundström, I.; Ekedahl, L.-G. A model of the Temkin isotherm behaviour for hydrogen adsorption at Pd–SiO₂ interfaces. *J. Appl. Phys.* **1997**, *82*, 3143–3146. [[CrossRef](#)]
19. Fogelberg, J.; Eriksson, M.; Dannetun, H.; Petersson, L.-G. Kinetic modeling of hydrogen adsorption/absorption in thin films on hydrogen-sensitive field-effect devices: Observation of large hydrogen-induced dipoles at the Pd–SiO₂ interface. *J. Appl. Phys.* **1995**, *78*, 988–996. [[CrossRef](#)]
20. Irokawa, Y.; Usami, M. First-Principles Studies of Hydrogen Absorption at Pd–SiO₂ Interfaces. *Sensors* **2015**, *15*, 14757–14765. [[CrossRef](#)]
21. Podlepetsky, B.I.; Kovalenko, A.V. Errors of Integrated Hydrogen Sensors based on FETs with Structure Pd-(Ag)–Ta₂O₅–SiO₂–Si. *J. Electrochem. Soc.* **2020**, *167*, 167524. [[CrossRef](#)]
22. Li, X.; Le Thai, M.; Dutta, R.K.; Qiao, S.; Chandran, G.T.; Penner, R.M. Sub-6 nm Palladium Nanoparticles For Faster, More Sensitive H₂ Detection Using Carbon Nanotube Ropes. *ACS Sens.* **2017**, *2*, 282. [[CrossRef](#)]
23. Penner, R. A Nose for Hydrogen Gas: Fast, Sensitive H₂ Sensors using Electrodeposited Nanomaterials. *Acc. Chem. Res.* **2017**, *50*, 1902–1910. [[CrossRef](#)] [[PubMed](#)]
24. Kim, H.; Yun, J.; Gao, M.; Kim, H.; Cho, M.; Park, I. Nanoporous Silicon Thin Film-Based Hydrogen Sensor Using Metal-Assisted Chemical Etching with Annealed Palladium Nanoparticles. *ACS Appl. Mater. Interfaces* **2020**, *12*, 43614–43623. [[CrossRef](#)] [[PubMed](#)]
25. Shin, W.; Hong, S.; Jung, G.; Jeong, Y.; Park, J.; Kim, D.; Lee, J.H. Improved signal-to-noise-ratio of FET-type gas sensors using body bias control and embedded micro-heater. *Sens. Actuators B* **2021**, *329*, 129166. [[CrossRef](#)]
26. Guo, S.Y.; Hou, P.X.; Zhang, F.; Liu, C.; Cheng, H.M. Gas Sensors Based on Single-Wall Carbon Nanotubes. *Molecules* **2022**, *27*, 5381. [[CrossRef](#)]
27. Usagava, T.; Takeyasu, K.; Fukutani, K. Hydrogen-Induced Dipoles and Sensing Principles of Pt-Ti-O gate Si-MISFET Hydrogen Gas Sensors. *Procedia Eng.* **2014**, *87*, 1015–1018. [[CrossRef](#)]
28. Usagava, T.; Daugherty, D. Semiconductor Gas Sensor. U.S. Patent 20160097731A1, 7 April 2016.
29. Sharma, B.; Sharma, A.; Kim, J. Recent advances on H₂ sensor technologies based on MOX and FET devices: A review. *Sens. Actuators B* **2018**, *262*, 758–770. [[CrossRef](#)]
30. Kumar, A.; Zhao, Y.; Mohammadi, M.M.; Liu, J. Palladium Nanosheet-Based Dual Gas Sensors for Sensitive Room-Temperature Hydrogen and Carbon Monoxide Detection. *ACS Sens.* **2022**, *7*, 225–234. [[CrossRef](#)]
31. Saxena, P.; Shukla, P. A Review on Gas Sensor Technology and Its Applications. In *Computational and Experimental Methods in Mechanical Engineering: Smart Innovation, Systems and Technologies*; Rao, V.V., Kumaraswamy, A., Kalra, S., Saxena, A., Eds.; Springer: Singapore, 2022; p. 239.
32. Available online: <http://ece723.tripod.com/lec04.pdf.p.20> (accessed on 15 February 2023).

Disclaimer/Publisher’s Note: The statements, opinions and data contained in all publications are solely those of the individual author(s) and contributor(s) and not of MDPI and/or the editor(s). MDPI and/or the editor(s) disclaim responsibility for any injury to people or property resulting from any ideas, methods, instructions or products referred to in the content.